INFACON 7, Trondheim, Norway, June 1995
Eds.: Tuset, Tveit and Page
Publishers: FFF, Trondheim, Norway

KINETIC SIMULATION OF THE CONTROL OF THE NITROGEN CONTENT OF LOW CARBON FERROMANGANESE IN A NOVEL COUNTER-CURRENT REACTION LAUNDER PROCESS

Lloyd R. Nelson*, David G.C. Robertson and K. Narayana Swamy
Center for Pyrometallurgy, Dept. of Metallurgical Engineering
University of Missouri-Rolla, Rolla, MO 65401-0249, U.S.A.
* Now Senior Process Engineer, Chromium R & D Department
GENCOR Process Research, Private Bag X10014,
Randburg, 2125, South Africa.

ABSTRACT

Control of the nitrogen content of low carbon (LC) ferromanganese (FeMn) through manipulation of the composition of bottom injected gases in a novel *C*ounter-*C*urrent *R*eaction *L*aunder (CCRL) Process was investigated. Substantial gas stirring (predicted to be above 9 Nm^3/t LC FeMn) is needed to promote metal-slag mass transfer in the proposed process, which involves counter-current refining of high-grade ferromanganese silicon with a lime-ore melt. In addition to the quantity of gas, the type of gas selected for bottom injection is important from both cost and metallurgical considerations. For nitrogen-'free' grades exclusive use of argon is almost unavoidable, but partial replacement with less expensive nitrogen becomes economically attractive if the content of dissolved nitrogen can be controlled to within acceptable levels. The *S*lag *M*etal and G*A*s *K*inetics (SMAK) program was used to study nitrogen absorption and desorption, and to predict the nitrogen level of LC FeMn alloy produced in a CCRL.

INTRODUCTION

Recently a novel CCRL process for production of refined LC FeMn (< 0.1 % C and < 1 % Si) was proposed, in which high-grade (> 26 % Si) ferromanganese silicon (FeMnSi) is contacted counter-currently with a lime-'ore' melt (manganese sinter + calcined lime) (Fig. 1) [1]. The fundamental refining reaction can be written as:

$$xSi + 2MnO_x = xSiO_2 + 2Mn \qquad (1)$$

(x = 1): $\Delta H°_{1600°C}$ = -137.6 kJ/mol Si; and $\Delta G°_{1600°C}$ = -90.9 kJ/mol Si [8]

$$K = a_{SiO2}{}^{x}.a_{\underline{Mn}}{}^{2} / a_{\underline{Si}}{}^{x}.a_{MnOx}{}^{2} \qquad (2)$$

This shows that the process is exothermic, so the use of hot liquid reactants should negate the need for an external process energy source; the addition of basic fluxes (lime) will drive the reaction to the right; and the use of manganese oxide in its lowest possible oxidation state ($x \approx 1$) will enhance the silicon utilization efficiency. The main requirements identified for such a lime-ore melt refining CCRL operation to be successful, were the need to:

- ensure the maintenance of strong driving forces for the refining reaction along the whole length of the reactor, requiring low extents of longitudinal mixing (represented by the

Inverse Peclet Number, $Pe^{-1} = D_e/uL$) in each liquid phase [2,3]; and,

- achieve adequate rates of interphase mass transfer (defined through the dimensionless CCRL Number for phase i, $(N_{CCRL})_i = (kA\rho/\dot{m})_i$ [1]) to promote the extents of the refining reactions.

k = Mass-transfer coefficient (m/s)
A = Interfacial area of phase i (m^2)
ρ = Density of phase i (kg/m^3)
$\dot{m}$ = Mass flow-rate of phase i (kg/s)
D_e= Eddy-diffusivity (m^2/s)
u = Velocity of flow of phase (m/s)
L = Length of reactor (m)

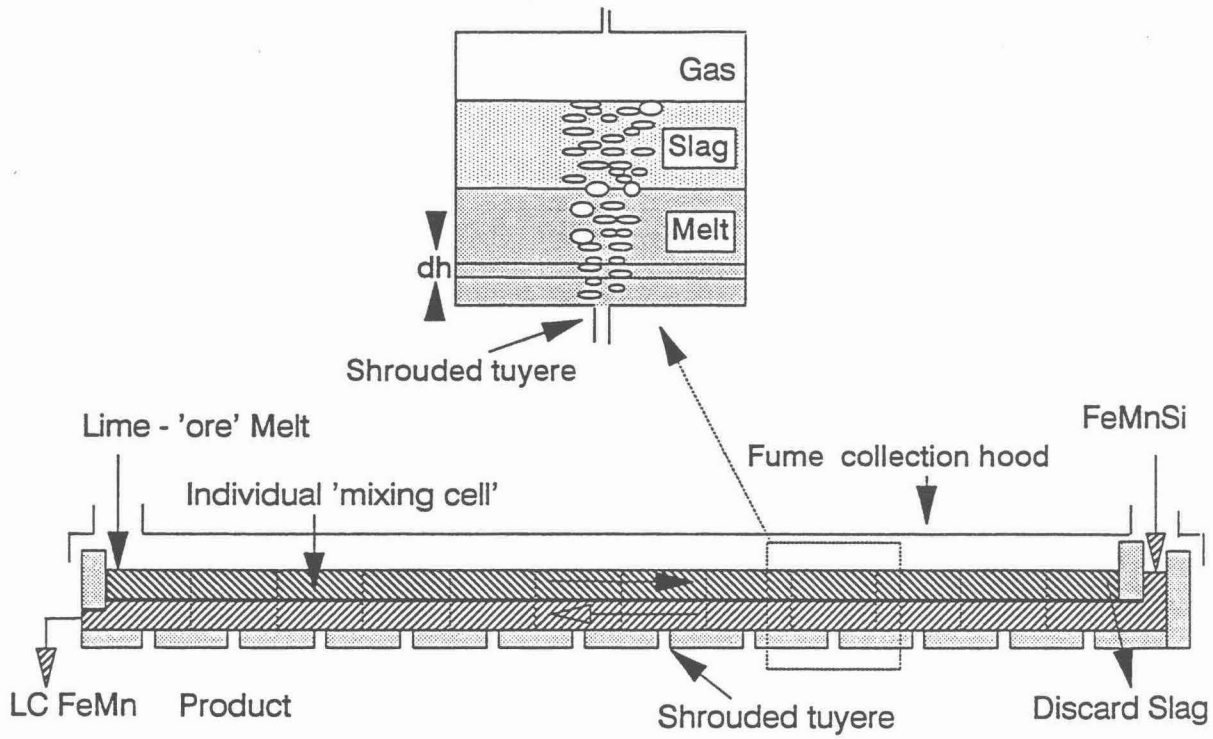

Estimated CCRL production rate of 50 000 tpa LC FeMn :
Approximate dimensions = 7m long x 0.7m wide x 0.7m liquid depth
Operating temperature = 1600°C

Figure 1 Schematic diagram of a CCRL for lime-'ore' melt refining of FeMnSi to LC FeMn, with a single transitory reaction cell highlighted.

The latter requirement is particularly important, as it defines:

- the quality of the final LC FeMn product in terms of alloy silicon content (and carbon content, by dilution with iron and manganese transferred to the alloy during refining of the silicon);
- the silicon utilization efficiency; and,
- the overall yield of manganese to the alloy.

Bottom injection of gas is a proven means to promote interphase transport. An additional benefit of gas injection, demonstrated by physical modelling of the CCRL, is that the extent of longitudinal mixing can be reduced dramatically ($D_e/uL < 0.1$) through appropriate bottom gas injection, using a single line of central tuyeres [2,3]. Earlier kinetic simulations using a steady-state, staged, counter-current model (which closely approximated plug flow behavior,

provided a sufficient number of stages was used) established that at least 9 Nm^3/t LC FeMn of gas was required to achieve the sufficient rate of mass transfer, to yield an acceptable process [1]. The focus of this work was on investigation of the effects that this predicted gas requirement has on the proposed CCRL Process for LC FeMn production.

The first issue is the selection of suitable gases for injection. In the highly reducing environment of the silicothermic refining process, nitrogen and argon are the only two industrial candidates. For economic reasons, industrial use of nitrogen (about \$0.2 / Nm^3) is strongly favored over that of argon (about \$0.9 / Nm^3) [4]. Nitrogen however, is highly soluble in liquid manganese alloys, and reacts with manganese in the solid state to form nitrides.

In the context of many commercial applications the presence of nitrogen in combination with manganese is desired, even to the extent that a suite of commercially nitrided grades of manganese has been developed, containing up to 4.5 % N [5]. It should be appreciated that the maximum solubility of nitrogen in liquid ferromanganese is only about 1.4 % N (at 1550°C - Fig. 2), so that simple bottom injection of nitrogen gas in the CCRL could never hope to directly yield a solidified LC FeMn product of the required nitrogen content. Such a CCRL product would however, represent an eminently suitable intermediate product for subsequent nitriding in the solid state to yield desired nitrogen grades.

In many other applications however, the presence of even minute traces of nitrogen is objectionable, and would be unacceptable to many steel, and stainless steel, end-users of LC FeMn. Two options exist to overcome this problem:
- costly total replacement of nitrogen with argon gas;
- cheaper, partial replacement of nitrogen with argon gas.

Prediction of nitrogen concentration profiles in the liquid alloy along the length of a CCRL, will be made for the following conditions:
- the case of nitrogen saturation in the alloy;
- steady-state absorption of nitrogen into the alloy during nitrogen injection; and
- steady-state desorption of nitrogen from the alloy (assuming a FeMnSi alloy initially saturated in nitrogen at the CCRL inlet) using argon gas (argon 'rinsing' of dissolved nitrogen).

The relative operating costs of these different scenarios will be given a cursory examination, and from this, coupled with the predicted alloy quality (in terms of nitrogen content), appropriate compromise solutions to the case of gas injection during production of refined LC FeMn in a CCRL will be presented.

KINETIC MODELLING OF NITROGEN ABSORPTION AND DESORPTION

Description of the SMAK Model

The generic SMAK software is a kinetic (mass transfer) model, which solves for thermodynamic equilibrium at each of the metal-slag, metal-gas and slag-gas interfaces, subject to the constraint of conservation of the fluxes of each element, where the fluxes are calculated according to a coupled reaction scheme. In the counter-current version of SMAK used to model the CCRL, the reactor length was conceptually broken up into a number of cells. The coupled reactions of each cell were then computed sequentially along the length of the reactor, for each counter-current liquid phase in turn, by a 'sweeping' procedure, until the final steady-state kinetic solution for the specified initial conditions of the CCRL was obtained.

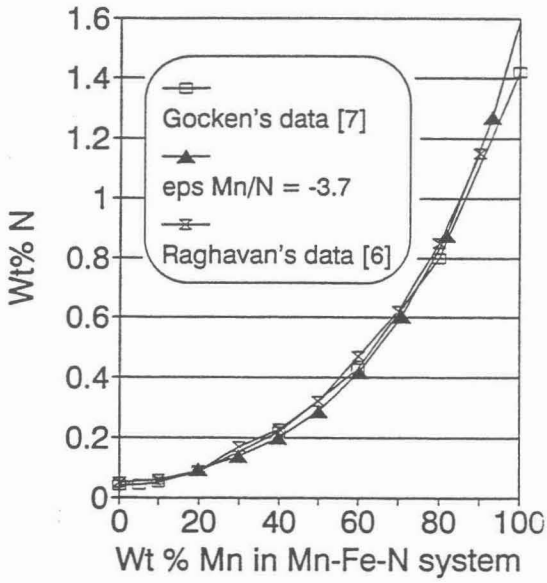

Figure 2 Measured and predicted solubilities of nitrogen in Fe-Mn at 1550 °C
eps Mn/N = ε_N^{Mn}

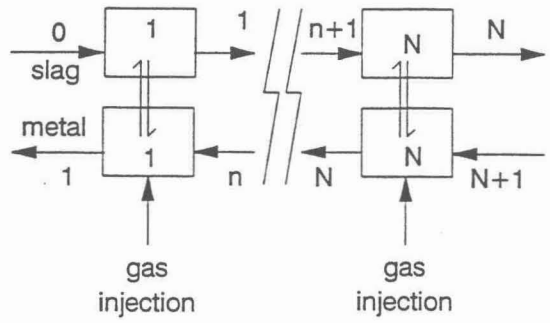

Figure 3 Schematic of the staged, 'plug flow' SMAK CCRL model

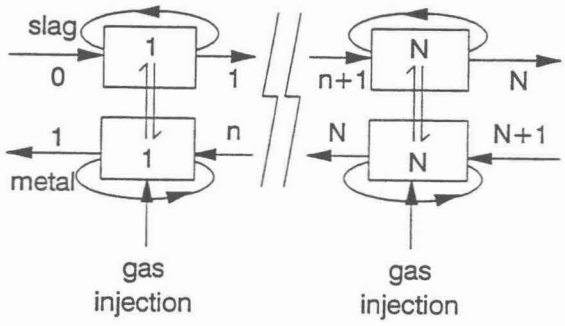

Figure 4 Schematic of the tanks-in -series SMAK CCRL model

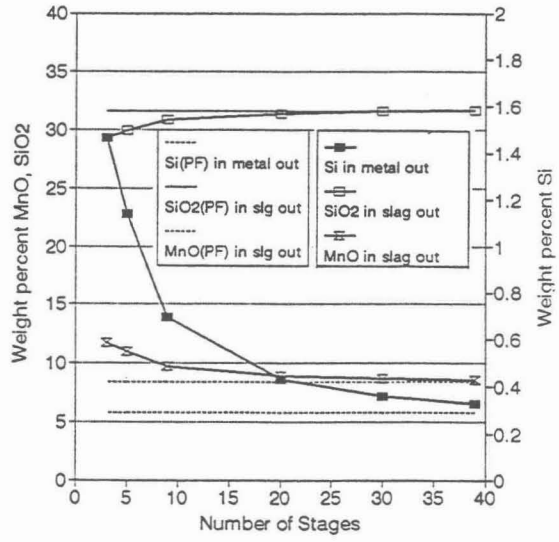

Figure 5 Comparison of results predicted by the 'plug flow' (PF) and tanks-in-series (TIS) SMAK models, as a function of the number of stages

i=	j= Solvent: Reference	Fe	Mn	C	Si	O	S	P	N
	First Order Terms:								
N	Fe (solvent): (6) #	-	-3.6*	-	-	-	-	-	-
	Fe (solvent): (9)	-	-	-	5.9*	4*	1.3*	6.2*	0.8*
	Fe (solvent): (8)	-	-4.5	7.2*	-	-	-	-	-
	Fe (solvent): (7)	-	-3	-	-	-	-	-	-
	Mn (solvent): (7)	3	-	-	-	-	-	-	-

Higher Order Terms:
Fe(solvent): P(N-Si) = 2.8

Note: * = Value selected for use in SMAK
= Regular solution approximation used to generate data at 1600 deg. C.

Table 1 Interaction parameter data (ε_i^j) of nitrogen in liquid iron manganese at 1600°C

Model Selection

A steady-state, staged kinetic model (Fig. 3) used previously to simulate the production of LC FeMn in a CCRL [1], gave results that approximated the ideal 'plug flow' conditions (provided that sufficient stages were used). This was expected to have overestimated the CCRL performance. Consequently a more realistic model involving the combination of a series of perfectly mixed tanks was developed (Fig. 4). An equal number of matching tanks (N) was used to model the metal and slag in this tanks-in-series (TIS) representation of the counter-current system. This was considered reasonable for the case of the bottom injected CCRL, as similar extents of longitudinal mixing were determined for both 'metal' and 'slag' phases in physical modelling of the CCRL [3]. The ideal of a perfectly mixed tank requires that the concentration of a phase leaving a tank is equal to the bulk concentration of that phase in the tank. A sufficiently large recycle stream (R, in units of mass flowrate) was initially defined for both phases to allow this requirement to be met, whereafter the correct mass flowrate of the recycle stream was computed, subject to the constraint of maintaining the volume of the tanks constant in each phase.

Transitory Model for Gas Bubble Reactions

In the TIS model of the CCRL, a transitory reaction model was developed to allow a more realistic computation of the reactions occurring at the gas-metal interface of bubbles rising up through the metal phase. This required dividing the metal phase into a number of conceptual height elements (dh), with the average gas pressure within a bubble being correctly calculated for the appropriate mean static head (due to overlying metal and slag) of a given height element (Fig. 1). This permitted the nitrogen concentration profile of the alloy along the length of the reactor to be more accurately predicted during both nitrogen absorption (nitrogen injection) and desorption (argon injection).

MODEL THERMODYNAMIC AND KINETIC DATA

Simulations based on any computer model are only as good as the available data. The thermodynamic and kinetic data used in the CCRL simulations have already been thoroughly reviewed [1]. An interaction parameter approach based upon manganese where possible, or otherwise iron, as the solvent, was used to model the alloy thermodynamics, while Gaye's model was used to model the slag thermodynamics. Only additional data pertaining to nitrogen are presented here.

Nitrogen Thermodynamic Data

Numerous data are available for nitrogen in iron systems, but a dearth of literature exists at compositions of manganese (over 90 % Mn) and silicon (up to 30 % Si, or mole fraction of silicon, X_{Si}, of 0.5) of interest here. Unfortunately no data are available for the specific quaternary Mn-Si-Fe-N system of real interest, so a number of assumptions had to be made to allow development of a thermodynamic representation of the behaviour of nitrogen in the alloy.

The LC FeMn product is well represented by the Fe-Mn-N ternary system. Raghavan [6] recently summarized the available data for nitrogen solubility (Fig. 2) from which it is clear that nitrogen has a substantially greater solubility in pure manganese (1.4 % N [7]) than in pure iron (0.47 % N [8]). Assuming iron to be the solvent, and using the reported value of $\Delta G^\circ = -1720 - 24.2T$ kJ/mol (for $2\underline{N} \rightarrow N_2$) [9], allowed a first order interaction parameter to be derived from the data, $\varepsilon_N^{Mn} = -3.6$ (Figure 2). This compared favorably with other reported data (Table 1) [7,8], and predicted a nitrogen solubility in good agreement with that reported for ferromanganese alloys over the entire composition range of interest (Fig. 2).

Unlike manganese, the presence of silicon strongly suppresses the solubility of nitrogen in iron, as indicated by the positive values of the ε_N^{Si} and ρ_N^{Si} interaction parameters for iron as the solvent (Table 1). In the absence of data for the interaction of dissolved nitrogen and silicon in manganese, the values for iron as the solvent were used in the current work. Interaction parameters available for iron as the solvent, were also used for the other species in the multicomponent alloy system (Table 1). This assumes ideality of the Mn-Fe system, which is reasonable in view of the data of Schultz et al. [10]. The wide discrepancy in the nitrogen solubility of the two pure elements does serve however, to show that the assumption of ideality is clearly only a convenient approximation.

Kinetic Data For Nitrogen

Kinetic data abounds for the Fe-N system, but only Inouye and Choh appear to have investigated the kinetics of nitrogen absorption and desorption in liquid iron containing manganese (up to 6.8 % Mn in iron, at 1600°C) [11,12,13]. A first order rate constant of 0.035 cm/s was reported for liquid phase mass transport control [11]. First order rate behavior, with liquid phase mass transfer as the controlling rate mechanism, has usually been observed in 'pure', surfactant 'free' iron (oxygen and sulphur contents well below 0.040 % O and 0.05 % S respectively) [11,14,15,16]. The unusually favorable thermodynamics of MnS formation, and the inherent deoxidizing nature of manganese are both conducive to the presence of few surfactants, so the application of the SMAK mass transfer model to simulation of the steady-state kinetics of nitrogen absorption and desorption in the CCRL alloy appeared vindicated. In the specific simulations presented for the bottom injected CCRL, $(N_{CCRL})_m$ = 21 was used ($(N_{CCRL})_s$ = 1.8), which corresponds to a high metal phase mass transfer coefficient of 0.095 cm/s.

RESULTS OF KINETIC SIMULATIONS

Tanks-in-Series Model Versus Original 'Plug flow' Model

The over-optimistic prediction of CCRL performance in the earlier work using the original 'plug flow' model [1], is demonstrated by the fact that a 27 % higher N_{CCRL} (N_{CCRL} = 1.8 compared to 1.41) was predicted as being necessary to achieve similar refining results on a nine-stage version of the TIS model (Fig. 5). Use of nine stages in the TIS model was prompted by the fact that it yielded an equivalent level of longitudinal mixing of D_e/uL = 0.0625 (from the expression $1/(N - 1) = 2\ D_e/uL$ [17]), which was almost identical to that reported in the metal phase of a number of top-lanced, counter-current WORCRA pilot-plant studies, ranging in capacities from 5 and 45 tph [18,19,20]. Increase in the N_{CCRL} to this higher level was assumed to be effected through increased gas injection from 0.016 Nm^3/s to 0.026 Nm^3/s), according to an expression developed by Richardson and co-workers in model studies of interfaces stirred by rising gas bubbles [21], and presented in the earlier CCRL work [1].

Predicted CCRL Performance

Provided that the selected level of bottom-gas injection into the CCRL indeed proves effective in achieving suitable high rates of interphase transfer, while simultaneously maintaining an acceptably low level of longitudinal mixing, a satisfactory CCRL performance was predicted (Fig. 6). The low alloy silicon and carbon contents (0.70 % Si and 0.040 % C respectively), the high silicon utilization efficiency (97 %) and the high recovery of manganese to the alloy (89 %) predicted are most favorable when compared to the known performance of alternative commercial refining processes available to produce

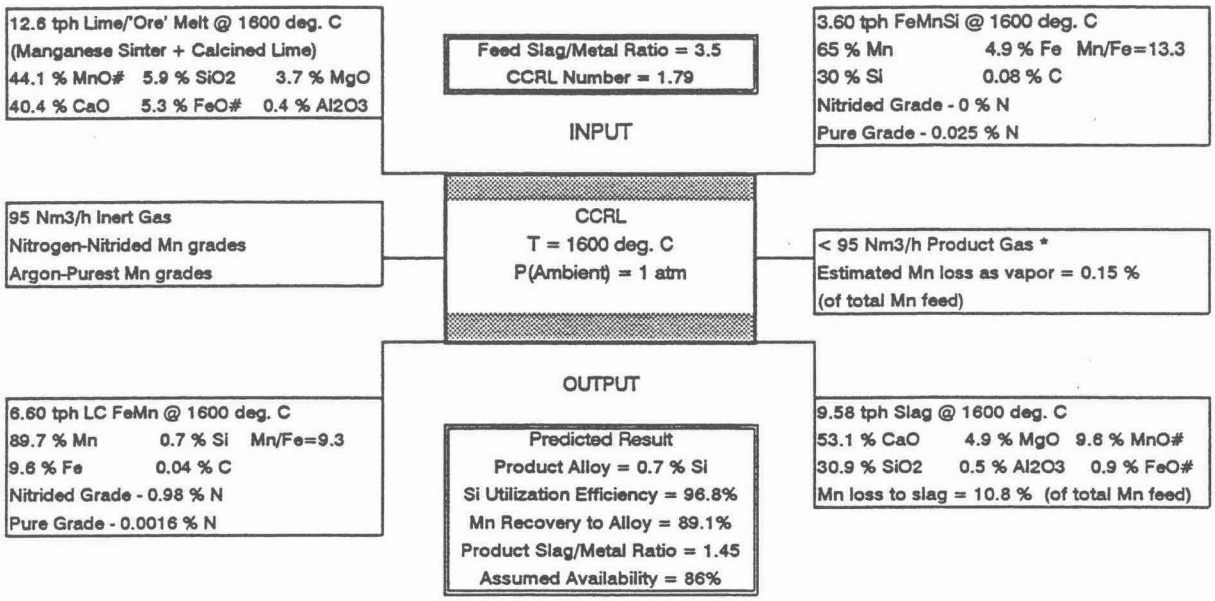

* During N absorption into metal, the vol. of injected gas decreases a lot as it rises through the metal.

Figure 6 Performance predicted by kinetic (TIS SMAK) simulation of a 9-stage CCRL, for production of 50 000 tpa LC FeMn.

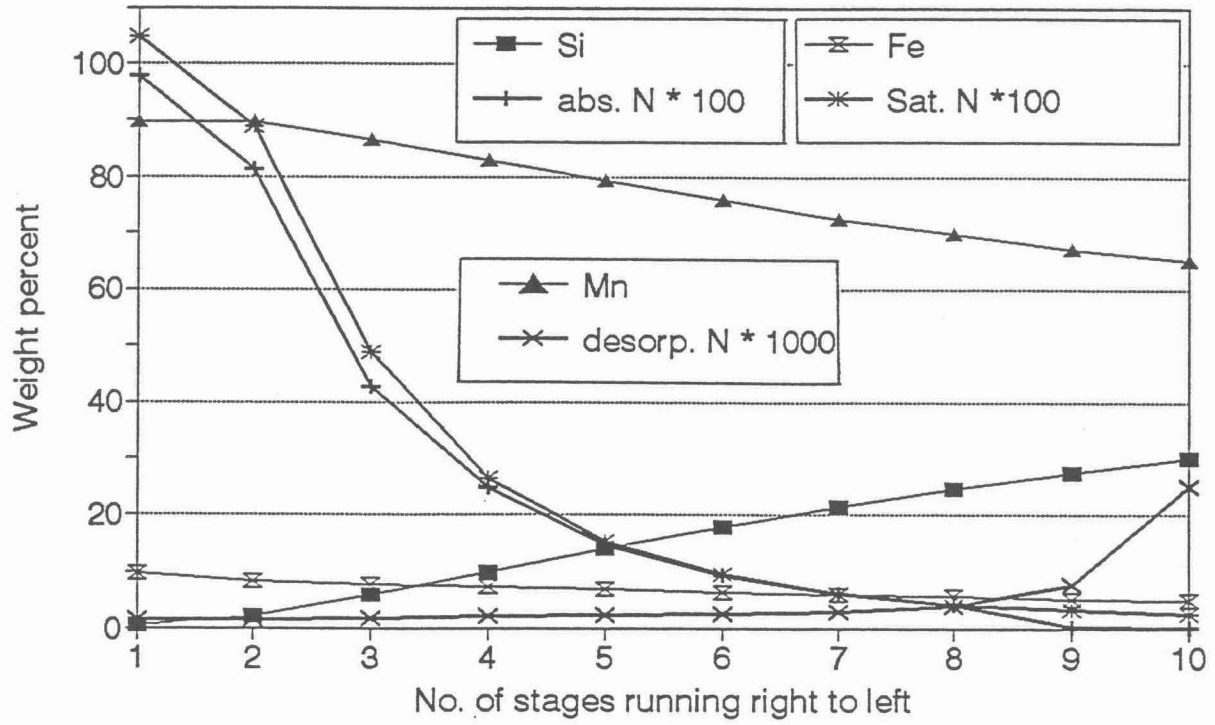

Figure 7 Plot of predicted alloy nitrogen content for saturation, absorption and desorption along the length of the CCRL

both medium carbon (MC) and LC FeMn, such as the Perrin Process [22], and batch pneumatic process [23,24].

Nitrogen Absorption

Simulation results using the transitory reaction TIS model of the CCRL during nitrogen injection, predict that a distinct steady-state concentration profile of nitrogen in the alloy will

develop along the length of the reactor (Fig. 7). At the FeMnSi feed end of the reactor, the high content of alloy silicon content (30 % Si, or X_{Si} about 0.5) is predicted to result in a rather low nitrogen content of 0.025 % N in the liquid alloy, as expected from the predicted solubility of nitrogen in the presence of abundant silicon. The nitrogen content progressively increases in the alloy in the direction of alloy flow, and is predicted to exit the CCRL at 0.98 % N. Because of the high absorption rate of nitrogen it was necessary to increase the nitrogen injection rate in the last two cells of the TIS model by a factor of three. This avoided almost complete absorption of the nitrogen injected. Comparison of the predicted nitrogen content profile with the projected equilibrium solubility of nitrogen in the alloy, clearly shows that the metal closely approaches saturation with respect to nitrogen under the conditions investigated (Fig. 7).

In applications where high nitrogen contents are desired (e.g., 200 series stainless steels), or can be tolerated, bottom injection of nitrogen gas at a rate of 14.3 Nm^3 /t LC FeMn would yield a commercially acceptable LC FeMn CCRL product. Such an alloy would also be eminently suitable as a nitrogen-bearing feedstock for subsequent gas-solid nitriding to yield an alloy of greater than 4 % N content, similar to the nitrided MC FeMn and nitrided electrolytic manganese grades available commercially [5].

Nitrogen Desorption

Total replacement of nitrogen with argon was simulated to investigate the potential for argon rinsing of the LC FeMn alloy. A starting nitrogen content of 0.025 % N, the saturation limit of the FeMnSi feed alloy, was assumed in simulations. Results showed that for the kinetically controlled steady-state case, a decreasing concentration of nitrogen was predicted to develop along the length of the CCRL (Fig. 7). The resulting product LC FeMn was predicted to contain as little as 0.002 % N, which would be acceptable to almost all end users of the ferroalloy. Of course the penalty for production of this alloy would be an increased operating cost for use of argon over nitrogen, estimated to be about $10 /t LC FeMn.

The high efficiency predicted for nitrogen desorption suggests that total replacement of nitrogen with argon may not be necessary. At the high FeMnSi feed end, bottom injection of nitrogen can probably be tolerated due to the reduced solubility of nitrogen in silicon containing alloys. Controlled staged replacement of the nitrogen with argon along the length of the reactor should be effective in limiting nitrogen absorption. In this way any nitrogen introduced into the alloy at its inlet to the CCRL is removed by argon rinsing just prior to its exit from the CCRL, to yield a refined low nitrogen-containing liquid LC FeMn. Such an alternative strategy of partial nitrogen replacement with argon should prove an economically attractive solution to yield LC FeMn of acceptably low nitrogen content for most commercial applications.

Manganese Vapor Losses

Results showed that a bubble rising up through the through the alloy progressively increased in manganese vapor content, until it became saturated with respect to manganese vapor. It was rather surprising therefore, that the manganese vapor loss was only reported to be 0.15 % of the total manganese input (Fig. 6). Three important factors act to limit the extent of manganese vaporization in the CCRL; namely,

- most of the gas injected into the reactor comes into contact with manganese of greatly reduced activity (the presence of silicon in the alloy dramatically lowers both the manganese mole fraction, X_{Mn}, and activity coefficient, γ_{Mn} [1]);
- the continuous nature of the CCRL (unlike current batch refining operations for MC FeMn production) means that only a small portion of the total quantity of gas injected actually comes into physical contact with alloy of high manganese activity (i.e., those injectors located near the LC FeMn product outlet);

- manganese only comes into contact with gas bubbles in the metal, where the higher total pressure of the gas (created by the static heads of overlying metal and slag) effectively lowers the mole fraction of manganese, so reducing the overall manganese vapor losses.

CONCLUSIONS

A new steady-state, transitory reaction, tanks-in-series kinetic (mass transfer) model of the CCRL showed that the level of gas injection required to achieve adequate rates of interphase mass transfer had previously been underestimated in a staged, 'plug flow' model of the CCRL. The revised predicted level of gas injection is 14.3 Nm^3/t LC FeMn, corresponding to a dimensionless $(N_{CCRL})_s$ of 1.8. Production of highly refined LC FeMn containing 0.70 % Si, 0.040 % C, with a 97 % silicon utilization efficiency, and at a 89 % overall recovery of manganese to the alloy is still predicted in this case, although the results clearly require verification by pilot plant work. The unusually low manganese vapor losses predicted for the CCRL contribute to high manganese yield, and are considered a highly desirable feature of the process, both for economic and environmental reasons.

Exclusive bottom injection with cheaper nitrogen gas is predicted to yield a liquid LC FeMn saturated in nitrogen, of 0.98 % N content, that should be acceptable to many end users of the alloy. In the case where nitrogen is an objectionable constituent, argon must be used to purge the alloy of nitrogen. Total replacement of the nitrogen with argon (with the CCRL fed by nitrogen saturated FeMnSi, 0.025 % N), is predicted to yield a liquid LC FeMn product containing as little as 0.002 % N. The increased operating cost associated with such use of argon gas is estimated to be significant, at $10 /t LC FeMn. Staged replacement of nitrogen with argon along the length of the reactor is suggested as the cheaper preferred alternative to yield LC FeMn of low nitrogen content, and could easily be simulated given sufficient interest

ACKNOWLEDGMENT

This research has been supported by the Department of the Interior's Mineral Institute Program administered by the U.S. Bureau of Mines through the gmtcp under grant number G1125229 2927.

REFERENCES

1. L.R. Nelson, et al., "Thermodynamic and kinetic simulation of a novel counter-current reaction launder (CCRL) process for the production of refined low carbon ferromanganese (LC FeMn)", Proc. of the EPD Congress 1994, T.M.S., (ed. G.F. Warren), San Francisco, Feb. 28 - Mar. 3, 1994, 713.

2. L.R. Nelson and D.G.C. Robertson, "Modeling of a counter-current reaction launder (CCRL) process for metal refining", Proc. of 77th Steelmaking Congress, Chicago, March, 1994, 665.

3. L.R. Nelson, et al., "Physical modeling of three-phase mixing in a counter-current reaction launder (CCRL) process for metal refining", submitted to Proc. of the EPD Congress 1995, T.M.S., Las Vegas, Feb. 12-16, 1995.

4. S. Hornby-Anderson and D. Rockwell, "Cost and quality benefits of carbon dioxide in the AOD", I&SM, Feb. 1993, 27.

5. Annual Book of ASTM Standards, Standard specification for electrolytic manganese metal, Designation A 601-69, and Standard Specification for ferromanganese, Designation A 99-82, 1990.

6. V. Raghavan, Phase Diagrams of Ternary Alloys, Monograph Series on Alloy Phase Diagrams, Part 1, 1987, 183.

7. R.A. Dodd and N.A. Gokcen, "Solubility of nitrogen in liquid-iron manganese alloys", Trans. T.M.S.-A.I.M.E., vol. 221, April, 1961, 233.

8. S. Ban-Ya and Y. Iguchi, Steelmaking Data Source Book, Gordon & Breach Science Publ., Revised ed., 1988.

9. C.H. Lupis, Chemical Thermodynamics of Materials, Elsevier Publ., 1983.

10. C.W. Schultz et al., "Activity of manganese in liquid iron-manganese alloys," U.S. Bur. of Mines, R.I. 6807, Nov., 1965.

11. M. Inouye and T. Choh, "Rate of absorption of nitrogen in liquid iron and iron alloys", Trans. ISIJ, vol. 8, 1968, 134.

12. M. Inouye and T. Choh, "Some considerations on the nitrogen transfer across gas-liquid interface", Trans. ISIJ, vol. 12, 1972, 196.

13. T. Choh, et al., "Kinetics of nitrogen desorption of liquid iron, liquid Fe-Mn and Fe-Cu alloys under reduced pressure, Trans. ISIJ, vol. 19., 1979, 221.

14. R.J. Fruehan and L.J. Martonik, "The rate of absorption of nitrogen into liquid iron containing oxygen and sulfur", Met. Trans. B, vol. 11B, Dec., 1980, 615.

15. M. Byrne and G.R. Belton, "Studies of the interfacial kinetics of the reaction of nitrogen with liquid iron by the ^{15}N-^{14}N isotope exchange reaction", Met. Trans. B, vol. 14B, Sept., 1983, 441.

16. Battle, T.P. and Pehlke, R.D., "Kinetics of nitrogen absorption/desorption by liquid iron and iron alloys", Ironmaking & Steelmaking, vol. 13, no. 4, 1986, 176.

17. O. Levenspiel and K.B. Bischoff, "Patterns of flow in chemical process vessels", Adv. Chem. Eng., 4, (eds. T.B. Drew et al.), Academic Press, 1963, 95.

18. T.W. Jenkins, et al., "Application of the Levenspiel dispersion model to metal flow in pilot plant WORCRA continuous steelmaking furnace", Met. Trans., 2, Apr., 1971, 1258.

19. T.A. Engh, et al., "A one-dimensional model of the WORCRA steel refining launder", Jernkont. Ann., 155, 1971, 553

20. S. Yamamoto, et al., "Refining of hot metal with soda ash in trough-type continuous refining furnace and fluid flow characteristics of hot metal and slag in the furnace", Tetsu-to-Hagané, 69, 14, 1983, 55.

21. F.D. Richardson et al., "Mass transfer across metal-'slag' interfaces stirred by bubbles," Phys. Chem. in Met. - Darken Conf., USS, 1976, 25-48.

22. Perrin, U.S. Patent 2,015,690, "Manufacture of iron alloys", Oct. 1, 1935.

23. D.S. Kozak and L.R. Matricardi, "Production of refined ferromanganese alloy by oxygen refining of high-carbon ferromanganese (MOR)," Elec. Furn. Conf. Proc., 1980, 123.

24. Uddeholm-Asea Fe-Mn converter, Met. Bull. Mon., no. 115, Jul., 1980, 71.